

Nanoscale Technique Prints Metal Films with Reusable Stamps and Tailored Surface Chemistry

Traditional nanolithographic techniques such as electron-beam or deep-UV nanolithography are limited to patterning small regions of specialized materials on rigid, ultraflat inorganic substrates. These restrictions are unacceptable for nascent applications in fields such as plastic electronics and biotechnology. Consequently, researchers are aggressively investigating alternative “soft lithography” methods, such as near-field phase-shift lithography, microcontact printing, and dip-pen lithography. In the July 15 issue of *Applied Physics Letters*, Y.-L. Loo and co-workers at Lucent Technologies described a nano-transfer printing (nTP) technique that is used to transfer metal films with features as small as 100 nm from the raised regions of a stamp onto substrates. This is reminiscent of woodcut printing, but on the nanometer scale. The high-resolution method is fast, can cover large areas, provides good adhesion, and is conducted under ambient conditions. Moreover, unlike its competing technologies, this soft lithography method is a one-step process and purely additive: It does not require any etching, resists, or post-patterning deposition.

The scientists produced rigid stamps by conventional patterning and etching of hard substrates such as glass or GaAs and created flexible stamps by casting a prepolymer of poly(dimethylsiloxane) (PDMS) in a patterned resist mold. They “inked” the stamp simply by evaporating the desired metal. Substrates can also be either rigid or conformal, and materials have included silicon dioxide and PDMS.

Intimate contact between the film and the substrate transfers the metal film through a common condensation reaction between hydroxyl (–OH) groups present on both surfaces. In order to accumulate the hydroxyl groups, the researchers applied either oxygen plasma or UV radiation to the native oxides.

This surface-chemistry restriction on the materials is not severe. Thus far, the researchers have successfully used nTP to print films of aluminum, whose surface spontaneously oxidizes, and, surprisingly, gold, after dusting it with titanium to obtain the requisite oxide layer.

“By exploiting other interfacial chemistries,” Loo said, “nanotransfer printing may be suitable for patterning a wide range of single- and multilayer conducting, dielectric, and semiconducting films.”

To appraise nTP’s potential application to plastic electronics, the scientists patterned

Au/Ti contacts and interconnects for organic transistors and complementary inverter circuits. The devices performed as well as top-contact devices fabricated with conventional shadow-mask gold electrodes.

RICHARD N. LOUIE

Diblock Copolypeptide Amphiphiles Form Rapidly Recovering Hydrogels

Protein-based hydrogels are used in a number of applications including drug delivery, tissue replacement, and cosmetics. Researchers at the University of California, Santa Barbara and the University of Delaware, Newark have synthesized diblock copolypeptides, composed of hydrophobic and hydrophilic domains, that form rigid hydrogels at very low concentrations (0.25–2.0 wt%). Gelation depends on the amphiphilic nature of the polypeptides as well as on the particular conformation of the hydrophobic domain. The porosity, thermal stability, and rapid recovery from network disruption make these materials attractive for a variety of biotechnological and biomedical applications.

As reported in a letter to *Nature* in the May 23 issue, a team led by University of California researcher Timothy J. Deming employed metal-mediated α -amino-acid N-carboxyanhydride polymerizations to control both the polypeptide chain lengths and composition of the amphiphiles. Poly(L-lysine-HBr) or poly(L-glutamate sodium salt), both highly charged polyelectrolytes at neutral pH, make up the hydrophilic blocks. The hydrophobic blocks are composed of poly(L-leucine) or poly(L-valine), which form rodlike α -helices and crystalline β -sheets, respectively. Copolypeptides of identical compositions to those that formed hydrogels but with random sequences did not form hydrogels at all.

Rheological measurements were made to investigate the nature of gel formation, the absolute strength of the gels, and the dependence of gelation on molecular parameters. The research team found that the hydrogels were one or more orders of magnitude stronger than an aqueous gelatin gel of the same weight percent. No visible thinning was observed up to 90°C; most protein gels generally start to dissolve at 60°C. No gelation occurs when the secondary structure (α -helix or β -strand) of the hydrophobic domain is precluded, either by incorporating a racemic mixture of amino-acid residues or simply by decreasing the degree of polymerization. This suggests that the self-assembly process is conformation-specific, similar to protein assembly, the

research team said. The addition of salt—for example, 25 mmol NaCl—weakens the gels, presumably through charge-screening of the polyelectrolytes. After large-amplitude oscillations were applied to break down the gel structure, recovery was probed by measuring the storage and loss moduli in the linear, small-deformation regime as a function of time. After about 10 s, the hydrogels recovered 80–90% of their strength, followed by a slower reorganization, after which the full initial storage modulus was restored. The researchers attributed this rapid recovery to the relatively low molecular mass of the copolypeptides, which enables them to reorganize quickly.

Gel morphology was visualized using cryogenic transmission electron microscopy (CTEM) and laser scanning confocal microscopy. Hydrogel formation appeared to coincide with the intergrowth of microscopically phase-separated domains of 1–25 μ m in size. CTEM visualization of the vitrified gel domains revealed a complex membrane assembly responsible for network formation at the nanoscale level. Gel porosity was verified with microrheological experiments, in which the Brownian motion of micrometer-sized tracer particles dispersed in the sample was measured. In a (L-lysine-HBr)₁₆₀(L-leucine)₄₀ gel, 0.5- μ m tracer particles diffused freely, while the motion of 1.0- μ m particles was restricted, which is taken as a measure of the lower size limit of the voids. This microscopic heterogeneity persisted after prolonged standing, heating, centrifugation, and bulk shear.

The researchers said that the very low mass fractions in these polypeptide gels, together with their microporous structure and recovery properties, may allow them “to fill...[a] unique niche between conventional polymer and surfactant hydrogels.” These gels also possess the “advantageous features of proteins, such as degradability and functionality, which [make] them attractive for biomedical applications,” said the researchers.

STEVEN TROHALAKI

Anode-Supported SOFC Performs Well at Intermediate Operating Temperatures with a Lanthanum Ferrite-Based Cathode

A group of researchers at Pacific Northwest National Laboratory in Washington has fabricated a strontium-doped lanthanum ferrite cathode that has a comparable performance with typical cathode materials, but at intermediate temperatures of 650°C to 750°C. A typical solid-oxide fuel cell (SOFC) configuration

employs a yttrium-stabilized zirconia (YSZ) electrolyte, kept thin (5–10 μm) to reduce ohmic losses at lower temperatures and supported by a planar Ni-YSZ anode (0.5 mm thick). However, cell performance of such SOFCs may suffer at intermediate temperatures because of the reduced electrochemical activity of the cathode. Researchers S.P. Simner, J.F. Bonnett, N.L. Canfield, K.D. Meinhardt, V.L. Sprenkle, and J.W. Stevenson investigated the use of La-ferrite and La-nickelate cathode compositions, rather than the much-researched La cobaltite, to facilitate matching of the coefficients of thermal expansion (CTEs) between the cathode and other cell components (thus enhancing thermal cycling characteristics) and to reduce chemical interactions. Cobaltites are well known for their high CTE and reactivity with YSZ to form electrically insulating zirconate phases.

As described in the July issue of *Electrochemical and Solid-State Letters*, the researchers prepared $\text{La}_{0.8}\text{Sr}_{0.2}\text{FeO}_{3-\delta}$ (LSF-20), $\text{La}_{0.7}\text{Sr}_{0.3}\text{Fe}_{0.8}\text{Ni}_{0.2}\text{O}_{3-\delta}$ (LSFN-3020), and $\text{LaNi}_{0.6}\text{Fe}_{0.4}\text{O}_{3-\delta}$ (LNF-6040) in addition to a mature interlayer material, $\text{Ce}_{0.8}\text{Sm}_{0.2}\text{O}_{1.9}$ (SDC-20) to be incorporated between the cathode and YSZ electrolyte. Sintering temperatures were optimized for each cathode: LSF-20 (1150°C for 2 h), LNF-6040 (1200°C for 2 h), and LSFN-3020 (1150°C for 2 h). Power densities were based on a screen-printed cathode with a diameter of 22 mm. Current-collection was achieved by the use of screen-printed platinum grids with embedded platinum gauze for the cathode and screen-printed NiO grids with embedded Ni gauze for the anode.

Despite its lower electrical conductivity, as compared with LNF-6040 and LSFN-3020, LSF-20 exhibited the highest cell performance at each temperature (850–950 mW/cm^2 at 750°C and 0.7 V). The researchers suggest that possible reasons for this result might be that LSF-20 has a greater activity for the reduction of oxygen or that its finer grain size can catalyze the reduction of oxygen through greater surface area. An interesting observation, unresolved at this time, is a power-density performance increase during the first 40 h of operation that levels off by 200 h and remains constant after that until the end of the test at 300 h. CTEs for the new cathode materials showed that LSF-20 had the best match with the anode while the others had slightly higher values. Thus, LSF-20 shows comparable performance to higher-temperature cathodes while resisting cell delamination by matching the CTE of the anode.

DONALD CARTER

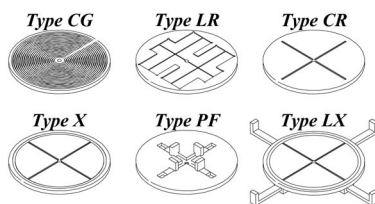
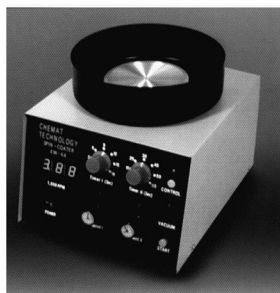
Magnesium Diffusion in Silica Enhanced by Na and Retarded by Al

Silica-forming ceramics can be beset by certain cations present in the ceramics either as impurities or as sintering additives. Both alkali and alkaline-earth cations are known to break the silica network structure, allowing nonbridging oxygen anions to form, thereby weakening the silica network. For example, researchers have learned that in NBD 200 silicon nitride, a commercial ball-bearing ceramic pressed with ~1 wt% magnesia, sodium impurities are responsible for increased oxidation, compared with other sodium-free magnesia-containing silicon nitrides.

Aluminum surface alloying by implantation results in a marked improvement in oxidation resistance in the NBD 200. This may be due to the ability of intermediate cations (including aluminum) to convert non-bridging oxygen anions back to bridging ones. Consequently, Priya Mukundhan and Henry Du at Stevens Institute of Technology, and Stephen Withrow at Oak Ridge National Laboratory, have implanted fused silica platelets with combinations of sodium, magnesium, and aluminum at room temperature to definitively study their interactions.

As reported in the June issue of the *Journal of the American Ceramic Society*, the

Cost-Effective Portable Spin Coater



Two-Stage Spinning

Dispense liquid during Stage 1
Spin-up and flatten during Stage 2

Adjustable Speed

Stage 1

500 to 2500 rpm
2 to 18 seconds

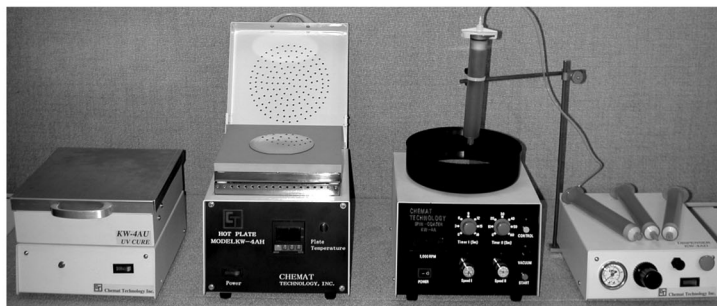
Stage 2

1,000 to 8,000 rpm
3 to 60 seconds

Vacuum Chucks

Wide Range of Vacuum Chucks
Available To Hold Different
Substrates in KW-4A Spin
Coater

KW-4A SERIES PRODUCT LINE



UV Curer
KW-4AC

Hot Plate
KW-4AH

Spin Coater
KW-4A

Dispenser
KW-4AD



CHEMAT TECHNOLOGY, INC.

9036 Winnetka Avenue, Northridge, CA 91324

1-800-475-3628, Fax: 818-727-9477

website: www.enlabproducts.com ; www.chemat.com

email: marketing@chemat.com

Circle No. 4 on Inside Back Cover